

DETERMINATION OF CALIBRATION FUNCTION FOR FATIGUE CRACK PROPAGATION BY MEASUREMENT SURFACE DEFORMATION

B. Glaser¹, N. Gubeljak², J. Predan² and P. Gubeljak³, A. Veg²

¹ Nuclear Power Plant Krško, Vrbina 12, SI-7800 Krško, Slovenia

² University of Maribor, Faculty of Mech. Eng. Smetanova 17, SI-2000 Maribor, Slovenia

³ High school International Bachelor, M. Zidanška 1, SI-2000 Maribor, Slovenia

Abstract: Components and structures exposed to elastic dynamic loading respond with elastic strains on the surface of the material. Mechanical response could be monitored by deformations on the surface. The measurements and monitoring of these parameters could be performed with electronic devices for on-line measurements, controlled by computerized systems. In the case of fatigue crack initiation and propagation the cyclic strain amplitude deviated from initial strain response (mean value and amplitude). Implementation of appropriate monitoring system supported by computerized programs for evaluation, analyses and activation represent important means to safe service component or construction. To evaluate flaw depth growth, the strain gauge measuring sensors could be used. These sensors measure surface deformation relaxation due to flaw depth growth. The monitoring of the material under cyclic loading could be performed with experimentally determined calibration curve, representing deformation on the surface and depth of the semi-elliptical crack growth on the surface or cross section of the material. The goal of this paper is describe electronic device and experimental procedure in order to determine calibration function.

Keywords: fatigue crack growth; surface deformation measurement

1 INTRODUCTION

The fracture mechanics approach for damage tolerance based on fatigue life in number of loading cycles consist of the fatigue initiation life of macroscopic crack size 1 mm in depth and subsequent fatigue crack propagation until the final fracture at critical crack length. The traditional approach provides number of cycles by integration of Paris-Erdogan crack growth relationship [1]:

$$\frac{da}{dN} = C\Delta K^m \quad (1)$$

Where m and C are material's constants, which depend on stress ratio R and environmental conditions for long fatigue crack behavior [1]. The stress intensity factor range ΔK is given by general equation:

$$\Delta K = Y \cdot \Delta\sigma_n \sqrt{\pi \cdot a} \quad (2)$$

Where Y is a function of crack size and crack shape (e.g. semi-elliptic surface crack or through thickness crack) and $\Delta\sigma_n$ is a nominal applied stress loading range, a is the crack length. In traditional approach the threshold stress intensity factor range ΔK_{th} is considered as constant for macroscopic visible cracks so called long cracks. The main part of fatigue life time belongs to microscopic crack initiation of short fatigue crack. The short crack effect occur until crack length depends on the effective stress ratio R , usually in range from 0.5 – 1 mm for structural steels. In this range of cracks the crack closure and other effects are not fully developed and threshold for fatigue crack propagation is lower than corresponding to long cracks for the same load ratio R , see Fig. 1. The Kitagawa and Takahashi diagram is used for fatigue crack initiation from surface or from notch, Fig. 2 [2].

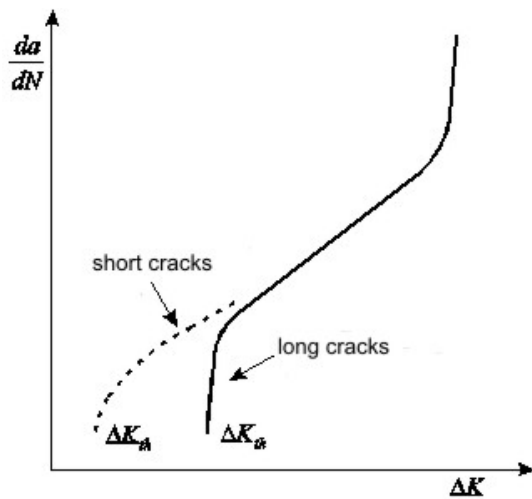


Figure 1: Fatigue crack growth rate vs. stress intensity factor range for short and long crack

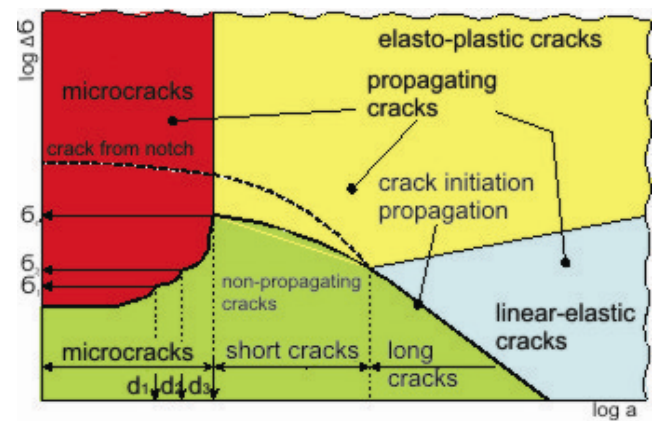


Figure 2: Fatigue crack propagation threshold as initiation from surface and from notch as function of crack length

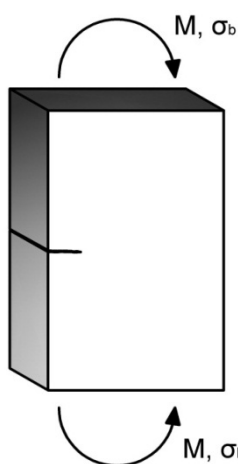
Figure 2 shows that threshold for crack initiation from the notch (dashed line) is higher than crack from the surface (solid line) in range of micro-cracks or short cracks. The fatigue threshold stress is function of crack length, as shown in Fig. 2. In case of fatigue crack initiation from the notch, the fatigue crack propagation becomes similar only in case of large crack. In this case the fatigue crack propagates only, if applied loading range is higher than fatigue crack propagation threshold:

$$\frac{da}{dN} = C \cdot (\Delta K^m - \Delta K_{th}^m) \tag{3}$$

The constants $m=3.01$ and $C=1,11 \times 10^{-14}$ (da/dN in mm/cycle and ΔK in $\text{MPa}\cdot\text{m}^{1/2}$) are determined experimentally by fatigue crack growth testing on tree point bend specimen of treated material, according to ASTM E647-05 standard [3]. The material threshold for crack propagation as function of the long cracks is defined by empirical equation in ref. [4] as:

$$\Delta K_{th-1} = -0.0038 \sigma_u + 15.5 \tag{4}$$

where σ_u is the ultimate tensile strength in MPa. In order to estimate fatigue crack growth rate the ΔK as function of crack length, the stress intensity function for a through thickness crack [5] has been used :



$$K_I = \sigma_b \cdot \sqrt{\pi a} \cdot Y \tag{5}$$

where Y is shape function

$$Y\left(\frac{a}{W}\right) = 1.122 - 1.40 \frac{a}{W} + 7.33 \left(\frac{a}{W}\right)^2 - 13.08 \left(\frac{a}{W}\right)^3 + 14 \left(\frac{a}{W}\right)^4$$

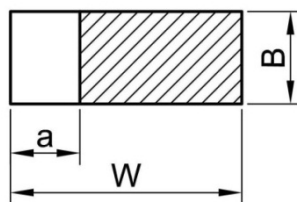


Figure 3: Stress intensity factor solution for Single edge surface crack in finite plate under bending loading

2 EXPERIMENTAL PREPARATION

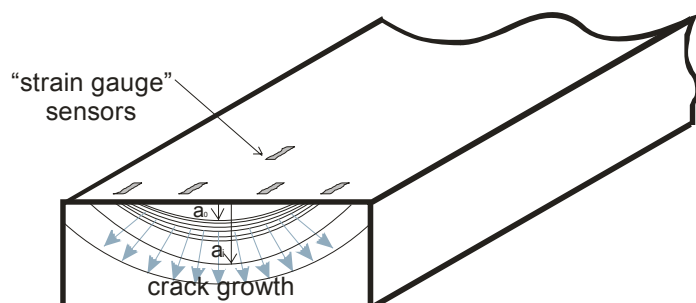


Figure 4: Schematic view of the strain gauges distribution and fatigue crack fronts of semi-elliptical cracks

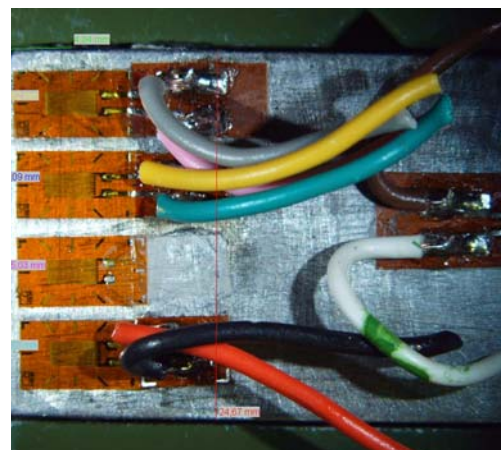


Figure 5: Measurement on specimen with strain gauges, right strain gauge is reference strain gauge at distance 38.9 mm

In order to estimate the fatigue crack propagation of crack from the surface notch, the experimental methodology is implemented for detection and monitoring of crack initiation and propagation by surface strain behavior. The multi-strain gauges technique (of 5 strain gauges) was implemented for the detection and monitoring of the crack initiation, as it is schematically shown in Fig. 4. Figure 5 shows photography with details of specimen, instrumented with multiple strain gauges.

The four point bend specimens were made of S690 steel grade with a yield stress of 695 MPa and tensile strength 854 MPa. Shell notched specimens were subjected to four bend cyclic loading with long span distance $S_1=200$ mm and short $S_2=90$ mm. Specimens were fatigue tested by using servo-hydraulic dynamic testing machine (INSTRON 1255) at frequency of 10 Hz, as shown on Figure 6. The position of strain gage sensors near the notch is essential for understanding of strain behavior. Sensors near the notch are affected with crack propagation differently that sensor at the balk of the specimen. Figure 7 shows the sensor position, while the typical strain lines on the surface during applied bending are shown in Fig. 8. Figure 8 shows also deviation of strain lines at the surface of specimens due to surface notch.



Figure 6: Four point bending fatigue testing of specimen with multiple strain gauges with Dynastrain device

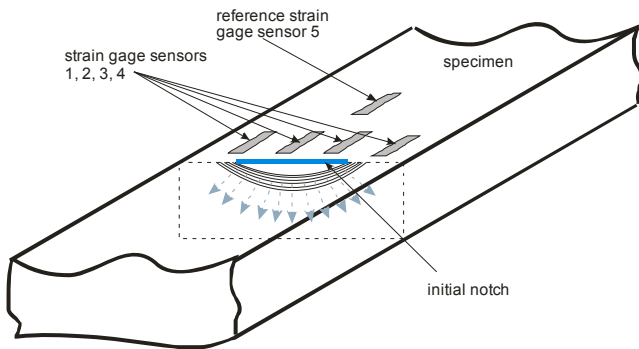


Figure 7: Strain Gage measure locations

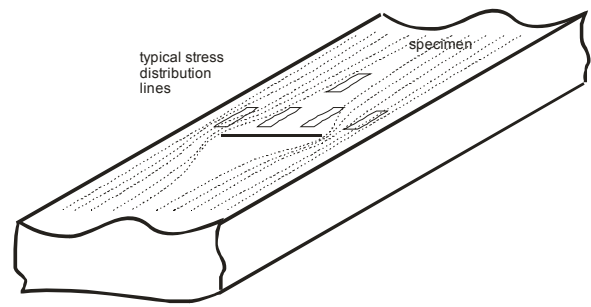


Figure 8: Surface distribution of stress

The electronic system for measurement of strain response during dynamic loading has been created as compact independent unit, supported by computer's software named "Dynastrain".

The measurement system consists of strain gage sensors, microcontroller system for sampling and data acquisition and amplification of measured values. The general descriptive block diagram is shown on Figure 9.

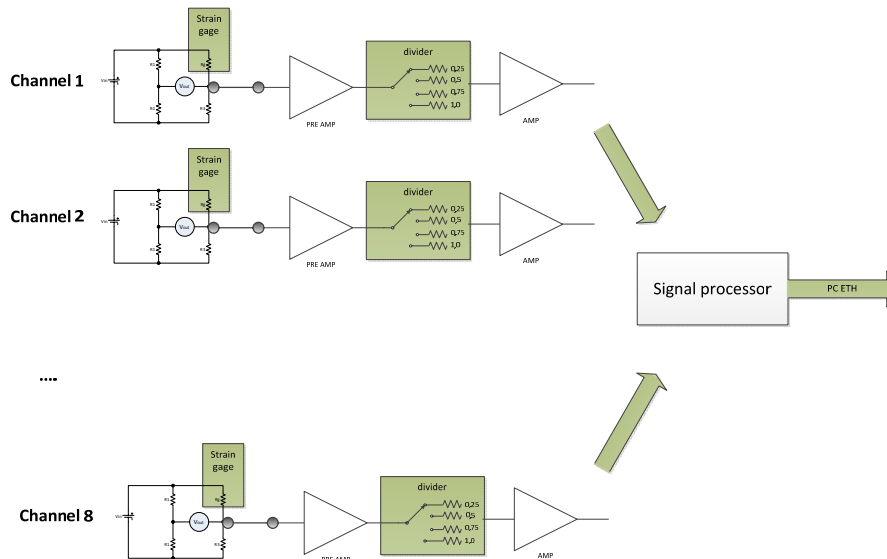


Figure 9: Dynastrain measurement block scheme

3 EXPERIMENTAL RESULTS OF FATIGUE TESTING OF SPECIMEN

The test procedure started with Dynastrain system calibration. The known applied force on specimen (used data from Instron hydraulic machine) was measured on Dynastrain channels. The reference channel was calibrated for F_{max} and F_{min} parameters with relative scale 0 to 100. Based on calculated stress, the read values from Dynastrain could be transferred to micro strain units. The main calibration was done on reference Strain gauge No. 5. The typical recorded characteristics in 1 second is shown on Fig 10.

The applied dynamic load was applied then sequentially with high amplitude of force F_{max} , $R=0.1$ for short number of cycles and lower amplitude forces for larger number of cycles. The amplitude of strains was collected each 1000 cycles, by aquisition frequency 900 samples per second. Tests were performed at ambiental temperatures by frequency of dynamic loading 10Hz for all regimes.

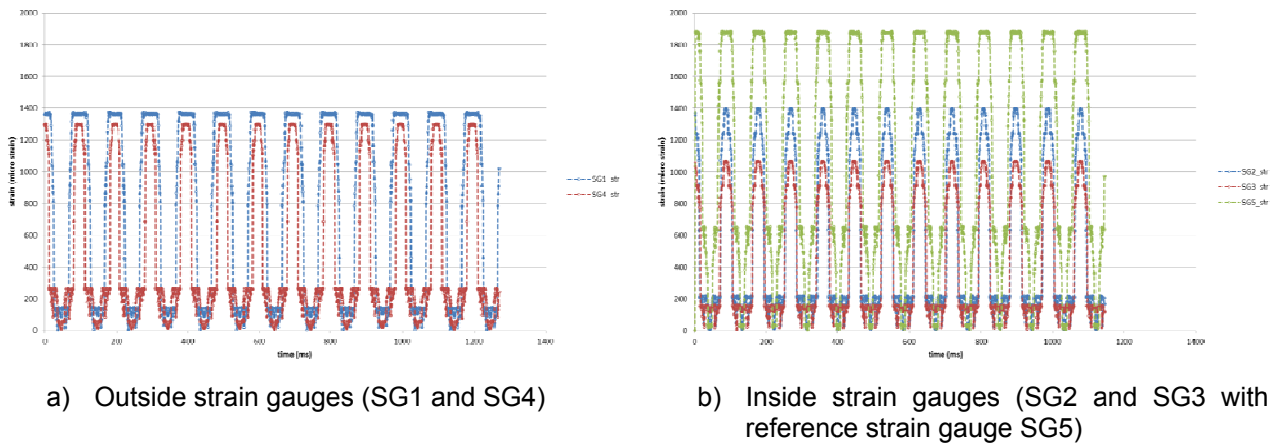


Figure 10: Typical response signals from Dynastrain in 1 sec during loading with $F_{max}=5$ kN

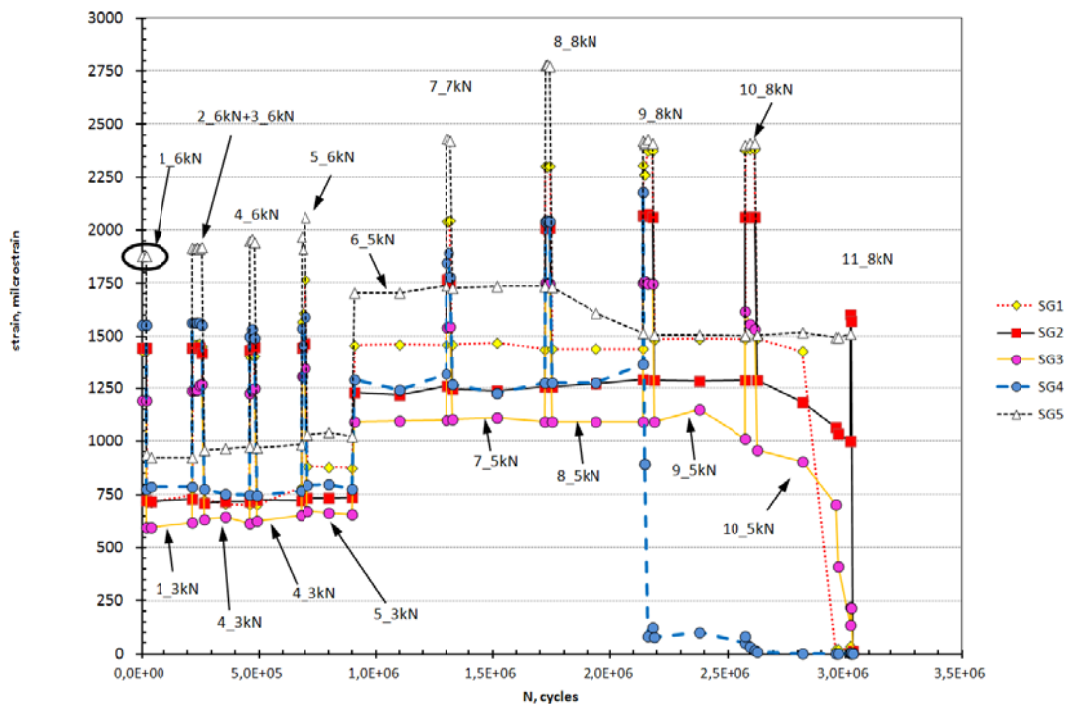


Figure 11: Performed fatigue loading with strain during each sequence of loading

Typical results from Dynastrain device are shown on Figure 10. The signals were not smooth sinusoid as applied by Instron hydraulic test device due to dynamic effects of strain gage fixation on the surface and noise at the 4 point fixation system. The main frequency and periodization remain as expected in line with applied loads. Each strain gauge has own characteristics of response regarding to their position from notch or crack. In this paper we are considering strain gauges No. 2 and No. 3 as relevant for recognition of crack growth and crack depth estimation.

Figure 11 shows performed fatigue regime with maximum forces. It is possible to recognize increasing of strain during fatigue under same maximum force $F=6$ kN. Each maximum force area has own strain range of loading. The strain starts to decrease with number of cycles after more than $1.8E+6$ of cycles. In order to apply uniform strain, the measured values is going to be divided by maximum stress.

4 ANALYSES OF RESULTS

The experiment assumption was, that stress distribution is likely to be equal at the position of reference sensor (SG5), and mostly affected on position of strain gauges (SG1-SG4) behind notch. Strain gauge No. 5 is reference sensor, because it's position is remote from notch and their strain amplitude will be less effected by crack extension than strain gauges (1-4) as sensors near the notch. We were assuming that at the beginning of bending the sensors were subjected to highest tension load, and consequently their cyclic

strain amplitude is higher. During the crack propagation their strain amplitude starts to decrease. The relationship between crack length and strain (amplitude and mean value) can be shown at points on the curve as so call calibration curve. With crack growth the strain is going to decrease. The exact crack length can be figured out by fractographic investigation in post-testing analyses. The relationship in form of curve as crack extension vs. number of cycle is so call crack growth curve. The calibration curve provides crack length regarding to strain change, as essential tool for establish on-line monitoring of dynamic loading components. The dynamic loading was conducted several times until final failure of specimens occurred at critical average crack length $a_c=6.96$ mm.

At the end of fatigue loading, the specimen was broken and fractographic investigation of fractured surface has been performed. The final crack length was measured in order to verify fatigue crack growth. The fractured surface of specimen is shown on Fig. 12. The fatigue crack growth was determined by using Paris fatigue relationship with same C and m parameters (Eq. 3) for whole crack propagation but different maximum loading. The obtained curve is given in Fig. 13. The detailed microscopic review of the break recognizes few typical locations of frontal lines during elliptical crack growth. The Figure 13 was created backwards, with starting at the last experimentally measured fatigue crack length. Since the number of cycles and crack extension are known, the parameters of crack growth equation C and m are used. The crack extension was obtained by integration of Eq. 3 for performed number of cycles. At each step of loading with higher loading amplitude shows steep increasing of crack growth until stage, where crack increment was too small. The higher fatigue growth rate appeared under shorter number of cycles but under higher loading amplitude. One can conclude that initiation stage for fatigue crack propagation starts around $1.3E+6$ of cycles, but strain starts to decrease after $1.8E+6$ of loading. It leads to two possibilities that fatigue crack starts to grow under higher number of cycles or strain gauges are not sensitive to crack initiation of short fatigue cracks because the SG are remote for more than 4 mm from the notch. However, during fatigue loading, the plastic zone at the crack tip appeared, where crack initiation process starts, as was explain in text book [6]. It makes difficult to distinguish start of fatigue long crack growth also. The fatigue cracks can also start growing in different points along the notch. It does not fit to model where only average crack length was considered by using given equations 1-5. The macro fatigue crack propagation and final failure appeared under higher fatigue loading level. Therefore, with presented technique is possible to estimate the number of cycles for initiation stage of creating fatigue crack. It is important fact in order to distinguish between crack initiation stage and macro fatigue crack propagation.

Since the Fig. 11 shows number of cycles vs. strain and crack extension, it is possible to create crack length vs. strain curve - so called calibration curve. Fatigue was performed with different amplitudes of applied forces. Since the fatigue loading is in elastic mode of material behavior, the measured maximal strain was normalized by applied maximum stress. The calibration curve (Figure 14) shows change of strain with crack propagation. SG4 at outside shows significant strain drop at the moment when crack pass the surface. There were just a few points recognized within this experiment, probably due to insufficient difference in amplitude of cyclic loading and same frequency applied at both sequences. At the same number of loading of cycles the strain also decrease at reference strain gauge (SG5) and slightly increased on opposite edge SG4 and SG2, as consequence of redistribution of strain on the surface of specimen.



Figure 12: Cross section of fractured specimen and location of strain gage sensors, magnification x5

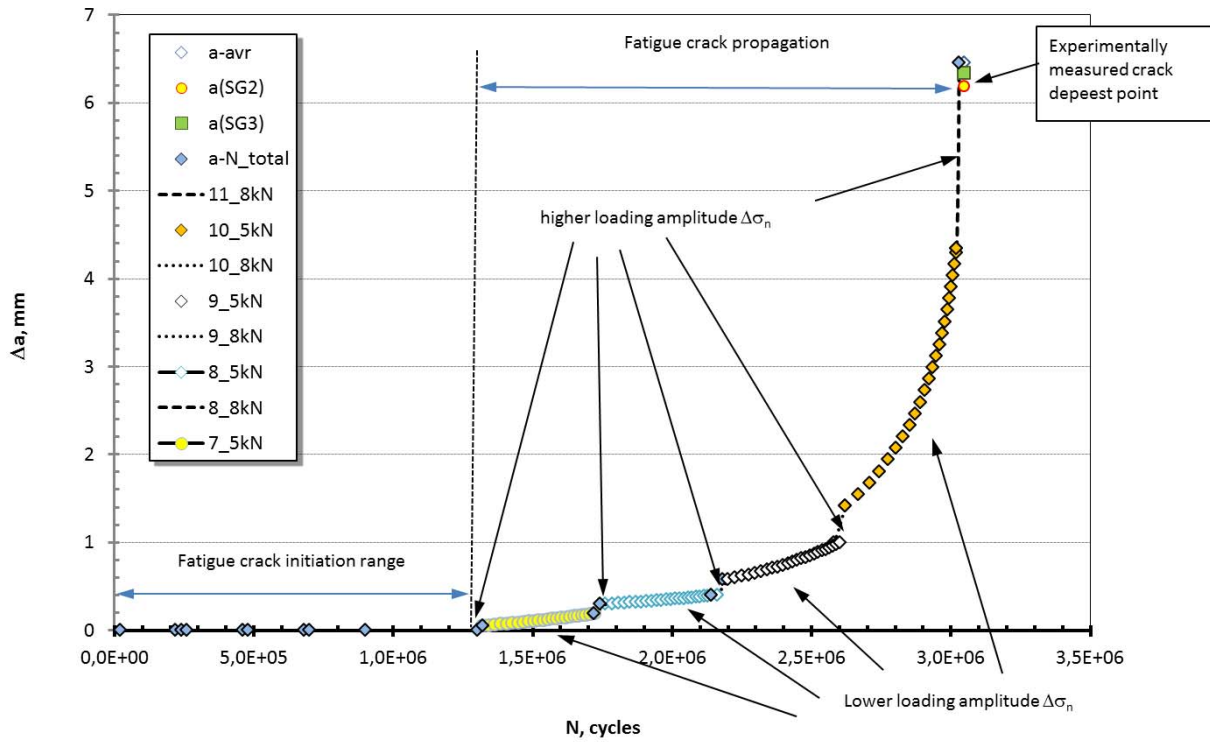


Figure 13: Fatigue crack growth curve

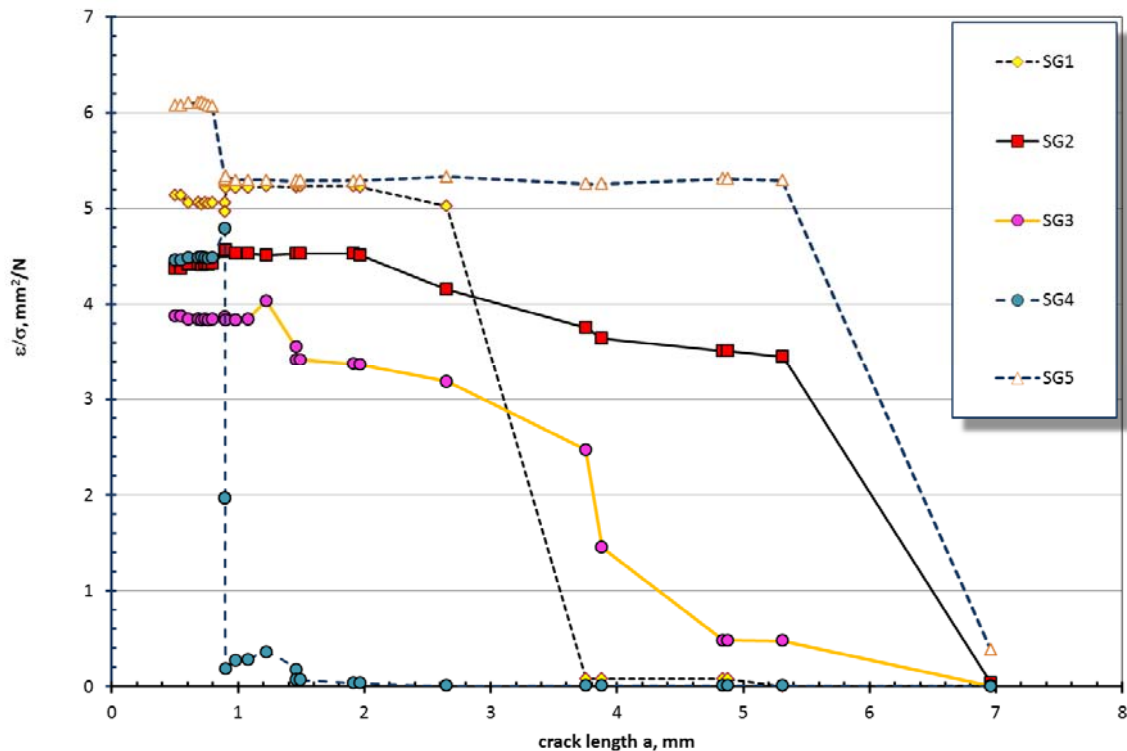


Figure 14: Calibration curve strain vs. crack length

Figure 14 also shows, that remote strain (measured by SG5) is not sensitive on crack extension to depth, because in range of crack length from 1 to 5.5 mm strain was similar. Figure 14 shows longer crack extension in points below SG3 (next to SG4) than SG2 and SG1. Therefore, we can assume that crack was propagated asymmetrically.

5 CONCLUSIONS

Paper presents technique for determination of calibration curve in term of strain-crack length during fatigue crack propagation on four point specimen. The technique is based on fatigue crack growth law and observation of strain amplitude change vs. number of loading cycles. In the case of different loading amplitude the strain should be normalized by applied stress. The strain redistribution occurred on the surface of specimen during the fatigue crack propagation. The strain redistribution is possible to be recognized as change of strain on SG, regarding to their position on the surface and crack location. The scenario of crack growth is possible to be determined in post-test analysis. The experimental results of strain monitoring show that sensitivity of strains on crack growth strongly depends on SG positions regarding to growing crack. It makes difficult to distinguish moment between initiation and fatigue crack propagation number of cycles. However, only the tentative number of cycles can be provided. Nevertheless, this experimental research and investigation demonstrate capability of continuous flaw growth measurement during the operation on critical places of the mechanical construction. In case of evident deviation from normal operating conditions, proper response is expected to prevent failure of the construction and prevention of failure.

6 NOMENCLATURE (OPTIONAL)

F	Force	N
σ	stress	$\frac{N}{mm^2}$
E	Young's Modulus	GPa
a	crack length	mm
ΔK	stress intensity factor	MPa
ϵ	deformation	mm/mm
$\frac{da}{dN}$	crack growth rate	mm/cycle

7 ACKNOWLEDGEMENTS

The authors would like to acknowledge the support of Nuclear Power Plant Krško d.o.o. for founding this research!

8 REFERENCES

- [1] Paris, P. and Erdogan, F., (1963), A Critical Analysis of Crack Propagation Laws, *Journal Basic Engineering*, pp. 528-534
- [2] Kitagawa H., Takahashi S., "Applicability of Fracture Mechanics to Very Small Cracks or the Cracks in the Early Stage" in *Proceedings of the Second International Conference on Mechanical Behaviour of Materials*, Boston, MA, 1976, pp.627-631
- [3] *ASTM E647-05 : Standard Test Method for Measurement of Fatigue Crack GrowthRate, Annual 2005*
- [4] Chapetti M.D., A simple model to predict the very high cycle fatigue resistance of steels, *Int. Journal of Fatigue* Vol. 33, (2011), pp. 833-841
- [5] Gross B., Srawley J.E., Stress intensity factor for single-edge-notch specimens in bending or combined bending and tension by boundary collocation of a stress function, NASA, Tech. Note, D2603, 1965
- [6] Anderson, T.L., *Fracture Mechanics - Fundamentals and Applications*, CRC Press, 1995